

## USP36 plays an oncogenic role in colorectal cancer cells

Lixiong LUO<sup>1,\*</sup>, Yijiang LI<sup>2,\*</sup>, Rongjie HUANG<sup>3</sup>, Ling LI<sup>4</sup>, Chuncai WU<sup>5</sup>, Qunzhang ZENG<sup>1,\*</sup>

<sup>1</sup>Department of Colorectal and Anal Surgery, Zhangzhou Municipal Hospital of Fujian Province and Zhangzhou Affiliated Hospital of Fujian Medical University, Zhangzhou, China; <sup>2</sup>Department of Radiation Oncology, Zhangzhou Municipal Hospital of Fujian Province and Zhangzhou Affiliated Hospital of Fujian Medical University, Zhangzhou, China; <sup>3</sup>Department of Small Intestine Surgery, Zhangzhou Municipal Hospital of Fujian Province and Zhangzhou Affiliated Hospital of Fujian Medical University, Zhangzhou, China; <sup>4</sup>Department of Reproductive Surgery, Zhangzhou Municipal Hospital of Fujian Province and Zhangzhou Affiliated Hospital of Fujian Medical University, Zhangzhou, China; <sup>5</sup>Department of Clinical Laboratory, Zhangzhou Municipal Hospital of Fujian Province and Zhangzhou Affiliated Hospital of Fujian Medical University, Zhangzhou, China

\*Correspondence: zqz134@sina.com

\*Contributed equally to this work.

Received June 29, 2023 / Accepted December 15, 2023

Cancer stem cells (CSCs) have emerged as crucial contributors to tumor relapse and chemoresistance, making them promising targets for treating cancers like colorectal cancer (CRC). However, the mechanisms governing CSC maintenance in CRC remain poorly characterized. In this study, we investigated the potential role of ubiquitin-specific protease 36 (USP36) in CRC. Our bioinformatic analysis revealed a significant upregulation of USP36 expression in CRC, and high USP36 levels were associated with poor prognosis in CRC patients. Furthermore, we observed an increase in USP36 expression in CRC cell lines. Knockdown of USP36 resulted in reduced viability, cell cycle arrest, increased apoptosis, and impaired migration and invasion in CRC cells. Additionally, the colony formation and sphere formation ability, as well as the expression of stem cell markers and pluripotent transcription factors, were substantially reduced in USP36-deficient CRC cells. These findings emphasize the role of USP36 as an oncogene in CRC, highlighting its potential as a therapeutic target for the treatment of CRC.

*Key words: colorectal cancer; cancer stem cell; USP36; knockdown; tumor progression*

Colorectal cancer (CRC) stands as one of the leading causes of cancer-related mortality worldwide [1]. It is more prevalent in developed countries, affecting more men than women [2]. Despite advances in treatment options, the five-year survival rate for patients diagnosed with CRC remains disappointingly low [3].

Emerging research has illuminated the presence of cancer stem cells (CSCs), an intriguing subpopulation of cells within the tumor microenvironment. These cells can self-renew and differentiate into various cell types, playing a critical role in the initiation, progression, and metastasis of various cancers, including CRC [4, 5]. CSCs are characterized by the expression of CD44, CD133, CD166, and epithelial cell adhesion molecule (EpcAM). They exhibit a remarkable 100-fold increase in their capacity for cancer initiation [6]. In CRC, CSCs have been specifically identified as CD133<sup>+</sup> or CD44<sup>+</sup> cells, and their presence has been associated with poor prognosis, as well as resistance to conventional radio-

therapy and chemotherapy [7]. The role of CSCs in CRC encompasses crucial aspects such as promoting angiogenesis, evading immune response, and fostering therapy resistance [8–10]. Furthermore, CSCs are believed to underlie tumor heterogeneity and recurrence [10, 11]. Understanding the biology and behavior of CSCs in the context of CRC represents a significant research area with the potential to yield more effective therapies.

Ubiquitin-specific protease 36 (USP36) belongs to the family of ubiquitin-specific protease (USP) enzymes, which play an important role in regulating protein degradation and turnover by removing ubiquitin from targeted proteins [12]. USP36's involvement extends to the regulation of various biological processes, including DNA repair, cell proliferation, and cell differentiation [13–15]. Stemness, characterized by the distinct properties of stem cells, such as self-renewal and differentiation potential into various cell types [16], is fundamental for tissue maintenance and organs repair throughout



the body. Stemness is tightly regulated by transcription factors, growth factors, and extracellular matrix components [17]. Recent studies have uncovered that USP36 interacts with and modulates the activity of key stemness-related signaling molecules, such as Wnt, thereby promoting self-renewal and pluripotency in stem cells [18, 19]. However, the role of USP36 in CRC is not fully understood.

In this study, we screened USPs that are upregulated in CRC tissues and identified multiple USPs whose expression is associated with the prognosis of CRC patients. Among them, USP36 is highly expressed in CRC cells and spheres. We performed a series of *in vitro* experiments to investigate the role of USP36 in regulating the viability, cell cycle, apoptosis, migration, and invasion of CRC cells. In particular, we measured the impact of USP36 deficiency on the stemness of CRC cells. Our data shed light on the function of USP36 in CRC.

## Materials and methods

**Datasets.** RNA-seq transcriptome information and corresponding clinicopathological information of CRC patients were obtained from TCGA GDC database, which serves as a comprehensive repository for cancer genomics data (<https://portal.gdc.cancer.gov/>).

**Survival analysis.** CRC survival analysis was conducted by employing the Kaplan-Meier (KM) estimate. The overall survival (OS) and disease-free interval (DFI) data were retrieved from TCGA-COAD cohort.

**Differentially expressed genes (DEGs) identification.** The DEGs between normal and tumor samples were identified by utilizing the R package “edgeR” (version 3.14) [20].  $|\log_2\text{FoldChange}| \geq 1$  and  $\text{FDR} < 0.05$  were set as the threshold for DEGs. A volcano plot was generated utilizing the R package “ggplot2”.

**Gene set enrichment analysis (GSEA).** GSEA was used to investigate the enriched KEGG pathways correlated with the expression of USP27X or USP36 in CRC using the GSEA software (version 4.2.1) (<https://www.gsea-msigdb.org/gsea/index.jsp>) [21].

**Cell lines.** CCD-841Con (No.IM-H477), HCT-116 (No.IM-H098), and LoVo (No.IM-H105) cells were obtained from Xiamen Immocell Biotechnology (China) and were respectively maintained in MEM, McCoy's 5A, and F12K medium (Immocell, China) supplemented with 10% fetal bovine serum (Gibco, USA) and 100 U/ml penicillin-streptomycin (Solarbio, China) in a humidified incubator at 37°C with 5% CO<sub>2</sub>.

**Plasmid.** Short hairpin (sh) RNAs targeting USP36, or non-targeting negative control was inserted into pLKO.1 vector and the resulting plasmids were named shUSP36 and shNC, respectively. The primer sequences are listed below: shUSP-6-1-F: 5'-CCGGCGAGTGTGATTCAGATCACTCTC-GAGAGTGATCTGGAATCACACTCGTTTTT-3'; shUSP-6-1-R: 5'-AATTAAAAACGAGTGTGATTCCAGATCAC-

TCTCGAGAGTGATCTGGAATCACACTCG-3'; shUSP36-2-F: 5'-CCGGTGCTGTGTGTCATG-CAGAACCCTCGAGGGTTCTGCATGACACACAG-CATTTTT-3'; shUSP36-2-R: 5'-AATTAAAAATGCTGTGTGTCATGCAGAACCCTCGAGGGTTCTGCATGACACACAGCA-3'; shUSP36-3-F: 5'-CCGGGAGCAA-ATATGTGTTGCTCAACTCGAGTTGAGCAACA-CATATTTGCTCTTTTT-3'; shUSP36-3-R: 5'-AATTAA-AAAGAGCAAATATGTGTTGCTCAACTCGAGTTGAG-CAACACATATTTGCTC-3'; shNC-F: 5'-CCGGTTC-TCCGAACGTGTCACGTCTCGAGACGTGACACGTTCCGAGAATTTTT-3'; shNC-R: 5'-AATTAAAAATTCTCCGAACGTGTCACGTCTCGAGACGTGACAC-GTTCCGAGAA-3'.

**RNA extraction.** The TRIzol-based (Invitrogen, USA) method was used to extract total cellular RNA. Briefly, 1 ml of TRIzol per 10<sup>7</sup> cells was added, followed by a 5 min incubation. Next, 0.2 ml of chloroform was added to each tube and vigorously vortexed for 15 s. Following this, the samples were centrifuged at 12,000× g for 15 min at 4°C, and the aqueous phase was carefully transferred to new RNase-free tubes. An equal volume of isopropanol was added to the aqueous phase and mixed well by inversion, and then incubated at room temperature (RT) for 10 min, followed by centrifugation at 12,000× g for 10 min at 4°C. Subsequently, the supernatant was carefully removed and the RNA pellet was washed with 1 ml of 75% ethanol, centrifuged at 7,500× g for 5 min, and air-dried for 10 min. Finally, the RNA pellet was dissolved in 20 µl of RNase-free water, and the RNA concentration was measured by Nanodrop (ThermoFisher, USA).

**Real-time quantitative PCR (RT-qPCR).** A cDNA synthesis kit (KR118; TIANGEN Biotechnology, China) was used to reverse transcription. Quantitative PCR was conducted on the StepOnePlus Real-Time PCR system (Applied Biosystems, USA), using a Fluorescent Quantitative PCR Assay Kit (FP209; TIANGEN Biotechnology) with the following primers: 18S rRNA-F: 5'-AGGCGCGCAAATTACCCAATCC-3'; 18S rRNA-R: 5'-GCCCTCCAATTGTTTCCTCGTTAAG-3'; USP36-F: 5'-AGCAGATGTCTGAGTGGAGAG-3'; USP36-R: 5'-GATGTTCTGTGGATGGTGAAGCG-3'; USP27-F: 5'-AGGCACTGCAAAGGTGATGA-3'; USP27-R: 5'-GTCCCAGCATGGGTCTATCG-3'; USP30-F: 5'-ACTAGGGTCCATCCTCTGGG-3'; USP30-R: 5'-GCACAAGCCCTTTTCTACGC-3'; USP38-F: 5'-CCACACTACTGCCTTCCCTG-3'; USP38-R: 5'-AGGGCTTGGGTCATACTTGC-3'; USP43-F: 5'-TGCACAGACAGCATTGCTATTATC-3'; USP43-R: 5'-GTAAACCGACAGACCTGGGTT-3'. The 2<sup>-ΔΔCT</sup> algorithm was used to calculate the relative expression of the target genes.

**Western blotting.** The cells were lysed on ice for 30 min using RIPA buffer supplemented with a phosphatase inhibitor (Beyotime Biotechnology, China), followed by sonication on ice for 10 min using Bioruptor. Then the samples were centrifuged to collect supernatants, and the protein concentra-

**Table 1. Antibodies for western blotting.**

Classification	Antibodies	Provider	Catalog NO.	Dilution
Primary antibody	Actin	Proteintech, China	20536-1-AP	1:5000
	USP38	Proteintech, China	18243-1-AP	13000
	USP30	Proteintech, China	10473-1-AP	1:2000
	USP36	Proteintech, China	10500-1-AP	1:3000
	OCT4	Proteintech, China	11263-1-AP	1:3000
	c-MYC	Proteintech, China	67447-1-Ig	1:2000
	Nanog	Proteintech, China	14295-1-AP	1:2000
	SOX2	Abclonal, China	A11501	1:2000
Secondary antibody	HRP-conjugated goat anti-mouse IgG	Proteintech, China	SA00001-1	1:10000
	HRP-conjugated goat anti-rabbit IgG	Proteintech, China	SA00001-2	1:10000

Abbreviation: HRP-horseradish peroxidase

tion was quantified using a BCA kit (PA115-02; TIANGEN Biotechnology, China). After being denatured at 95 °C for 10 min, the samples were loaded into 4–16% SDS-PAGE gels (20 µg protein/well). Electrophoresis was 1.5 h at 90 V and electrophoretic transfer for 1.5 h at 350 mA. Subsequently, the PVDF membranes were blocked with 5% non-fat milk for 1 h, followed by incubation with primary antibody solutions overnight at 4 °C. Afterward, the membranes were washed with TBST and then incubated with secondary antibody solutions for 1 h at RT. Finally, the membranes were washed with TBST three times washes and incubated with the working solution from an ECL kit (Bio-Rad, USA) and the signal was visualized and documented using a Bio-Rad ChemicDoc machine. The band intensity was quantified with ImageJ (NIH, USA). The antibodies used for western blotting are listed in Table 1.

**Spheroid formation assay.** Cells were plated at a density of 2,000 cells/well in ultralow attachment plates (CLS3471, Corning, USA). HCT-116 and LoVo cells were respectively cultured for ten days in Immocell's McCoy's 5A or F12K medium supplemented with 4 µg/ml insulin (HY-P73243, MedChemExpress, USA), 1:50 B27 (17504044, Gibco, USA), 20 ng/ml epidermal growth factor (E9644, Sigma, USA), and 20 ng/ml basic fibroblast growth factor (F9786, Sigma, USA). The passage of primary spheres was conducted by digestion with 0.25% trypsin and resuspension in MEM or F12K medium with the above supplements. Sphere counting was performed under a microscope. The experiments were performed in triplicates and the data are presented as the mean ± SD.

**Methyl thiazolyl tetrazolium (MTT) assay.** MTT assay was employed to assess cell viability. Briefly, cells transfected with shNC or shUSP36 for 48 h were seeded into 96-well plates at a density of 5,000 cells/well. Subsequently, A final concentration of 0.5 mg/ml of MTT reagent (Yeasen, China) was added to each well and incubated for 4 h at 37 °C. Afterward, the medium was removed and 100 µl dimethyl sulfoxide (Sigma, USA) was added to incubate for 4 h in the dark. Finally, the OD<sub>540</sub> values were measured by a microplate reader.

**Annexin V/PI staining.** Apoptosis was assessed by Annexin V/PI staining using an Annexin V-FITC kit (Beyotime Biotechnology, China), following the manufacturer's instructions. Briefly, HCT-116 and LoVo cells were collected and washed with PBS. Annexin V-FITC staining solution, PI staining solution, and binding buffer were then added to the cells with gentle pipetting. After 20 min of incubation in the dark, the cells were subjected to flow cytometry, and the data were analyzed with FlowJo software (version 10.8.1).

**7-amino-actinomycin D (7-AAD) assay.** The cell cycle was determined by the 7-AAD assay. Cells were digested with 0.25% trypsin/EDTA and fixed in pre-chilled 95% ethanol at -20 °C for 12 h. Subsequently, cells were washed with PBS and incubated with 20 mg/ml 7-AAD (Beyotime Biotechnology, China) in PBS at 37 °C for 10 min. Finally, cells were measured by flow cytometry, and the data were analyzed using FlowJo software (version 10.8.1) with the Watson pragmatic curve fitting algorithm.

**Transwell assay.** For the Transwell migration assay, HCT-116 or LoVo cells transfected with the indicated plasmids were resuspended in a serum-free medium and seeded into the upper chambers of the Transwell plates (8 µm, Corning, USA) at a density of 5×10<sup>4</sup> cells/well. Each lower chamber was filled with 600 µl RPMI-1640 medium supplemented with 10% FBS and 100 U/ml penicillin-streptomycin. After an incubation period of 24 h at 37 °C, the upper chambers were washed with PBS and fixed with 95% ethanol for 10 min, followed by staining with a 0.1% crystal violet solution for 10 min. Finally, the stained cells were washed with PBS, air-dried, photographed, and quantified using ImageJ (NIH, USA). For the invasion assay, the experimental procedures were identical except the upper chambers were coated with 100 µl 1:8 diluted Matrigel (BD Sciences, USA) for 12 h at 37 °C.

**Statistical analysis.** Bioinformatics analysis was performed using R (v.4.0.5). The correlation was analyzed by Spearman's Rank-Order Correlation coefficient. Bar graphs were generated by Prism 8.0 (GraphPad, USA). Unpaired two-tailed Student's t-test was applied to calculate the signifi-

cance between two data sets. A p-value  $<0.05$  was considered statistically significant.

## Results

**USP36 is overexpressed in CRC tissues and predicts poor prognosis of CRC patients.** To identify overexpressed USPs in CRC tissues, we analyzed the expression of 56 USPs in TCGA-COAD cohort. We observed multiple USPs that are differentially expressed between non-tumor (NT) tissues and CRC tissues (Figure 1A). Among them, the expression of USP27X, USP31, and USP36 were significantly upregulated in CRC tissues compared to NT tissues (Figure 1B). We then investigated the correlation between the expression of USP27X, USP31, and USP36 and OS or

DFI of CRC patients. The KM curves showed that high levels of USP27X and USP31 are not significantly associated with the OS of CRC patients (Figures 1C, 1D) but are linked to a higher probability of DFI (Figures 1F, 1G). By comparison, overexpressed USP36 predicts worse clinical outcomes in terms of OS and DFI (Figures 1E, 1H). In addition, GSEA analysis data indicated that USP36 expression is significantly associated with the Notch and Hedgehog signaling pathways (Figures 1I, 1J). Taken together, these results suggest that USP36 is overexpressed in CRC tissues and associated with poor prognosis of CRC patients.

**USP36 expression is elevated in adherent CRC cells and CRC cell spheres.** Next, we evaluated the expression of USP36 in colon epithelial cell line CCD-841Con and CRC cell lines HCT-116 and LoVo. RT-qPCR and western blotting

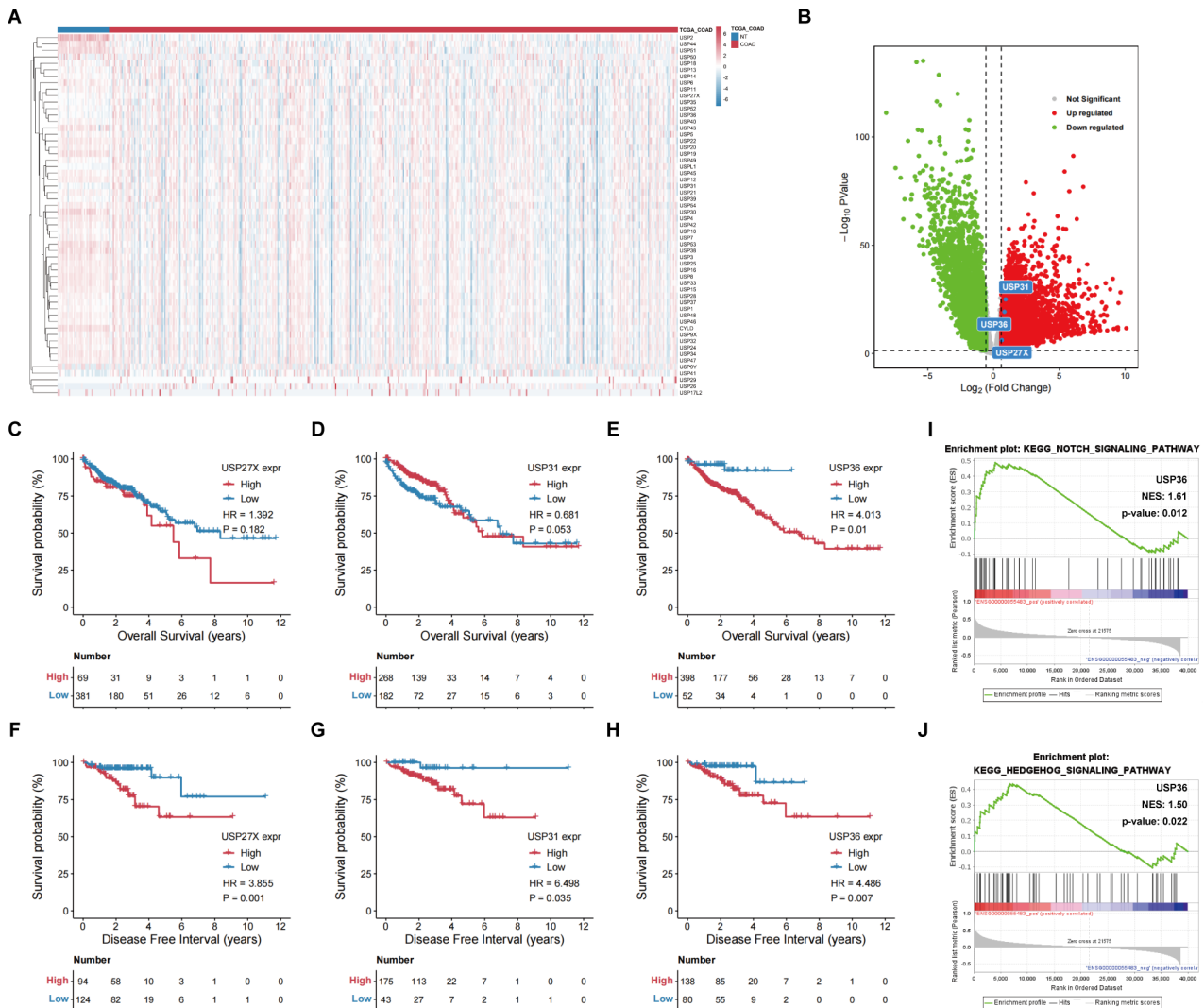


**Figure 1.** The association between USP36 expression and CRC prognosis. A) Heatmap showing the relative mRNA expression of the indicated USPs in NT and CRC tissues from TCGA-COAD cohort. B) Volcano plot displaying the DEGs between NT and CRC tissues from TCGA-COAD cohort. C–E) The KM curves depicting the OS of the CRC patients predicted by high and low expression of USP27X, USP31, and USP36. F–H) The KM curves indicating the DFI of the CRC patients predicted by high and low expression of USP27X, USP31, and USP36. I–J) GSEA plots showing the enriched KEGG pathways associated with the expression USP36 in CRC patients.

results indicated that USP36 expression is significantly higher in both CRC cell lines than in CCD-841Con cells (Figures 2A–2C). To determine whether USP36 expression is related to the stemness of CRC cells, we induced the HCT-116 cells to form spheres, a model that is widely used to study the properties of stem cells and CSCs [22–24]. RT-qPCR results revealed that USP36 is one of the USPs that are highly expressed in HCT-116 spheres (Figure 2D). Notably, the expression of the top 5 highly expressed USPs, including USP30, USP27, USP36, USP38, and USP43, was substantially increased in HCT-116 spheres compared to adherent HCT-116 cells, as indicated by RT-qPCR data (Figure 2E). In line with this, western blotting data confirmed that the protein levels of USP36, USP30, and USP38 were upregulated in HCT-116 spheres compared to adherent HCT-116

cells (Figures 2F, 2G). Collectively, these findings indicate that USP36 may play a role in regulating the activity and stemness of CRC cells.

**Knockdown of USP36 resulted in reduced viability, cell cycle arrest, increased apoptosis, and mitigated migration and invasion in CRC cells.** To determine the function of USP36 in CRC cells, we began with the knockdown of USP36 in HCT-116 and LoVo cells. RT-qPCR and western blotting results showed that all three shUSP36s efficiently depleted USP36 in both CRC cell lines (Figures 3A–3C), and we selected shUSP36-2 in the subsequent experiments. We then performed MTT assays and observed that the viability of CRC cells was significantly reduced upon USP36 deficiency (Figure 3D). Furthermore, 7-AAD staining data revealed that USP36 deficiency induced G0/G1 phase arrest in both LoVo

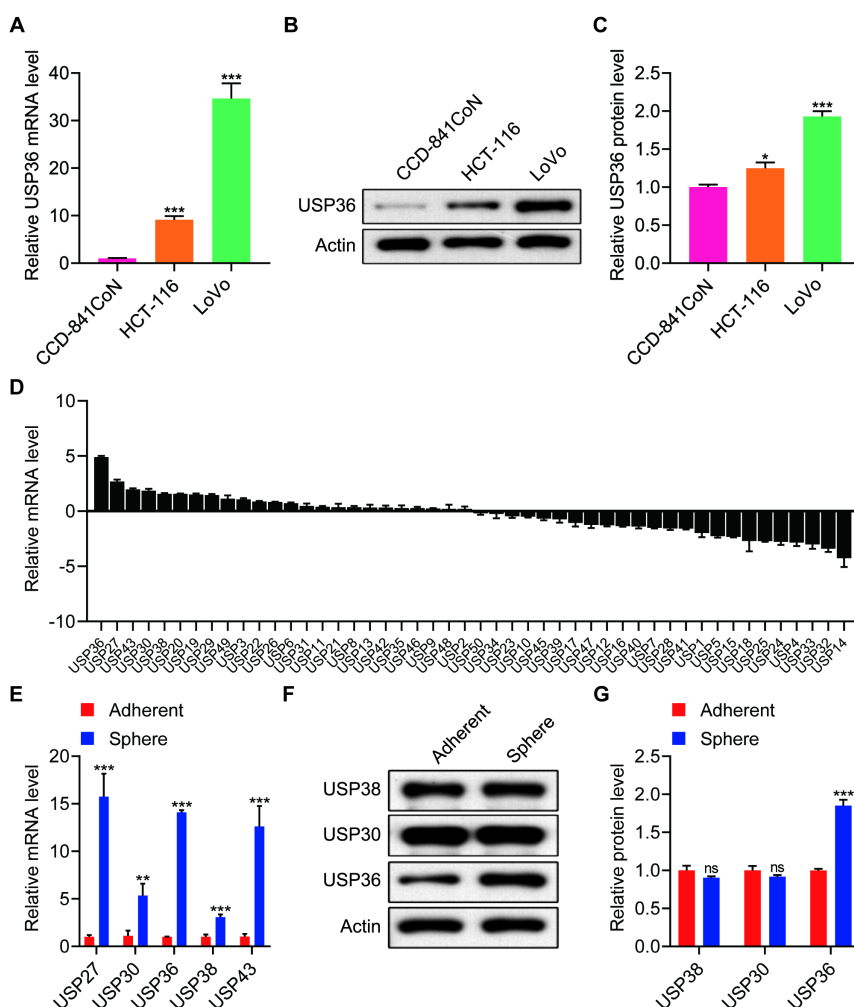


**Figure 2.** USP36 expression in CRC cells and CRC spheres. **A)** RT-qPCR data showing the expression of USP36 in the indicated cell lines. **B)** Western blotting results indicating the expression of USP36 in the indicated cell lines. **C)** Quantification of the data in **B**. **D)** RT-qPCR data depicting the relative mRNA expression of the indicated USPs in HCT-116 spheres. **E)** RT-qPCR data illustrating the mRNA expression of USP27, USP30, USP36, USP38, and USP43 in adherent HCT-116 cells and HCT-116 spheres. **F)** Western blotting outcomes showing the expression level of USP38, USP30, and USP36 in HCT-116 spheres. **G)** Quantification of the data in **F**. \* $p < 0.05$ , \*\* $p < 0.01$ , \*\*\* $p < 0.001$ , \*\*\*\* $p < 0.0001$

and HCT-116 cells (Figures 3E, 3F). Additionally, Annexin V/PI staining outcomes indicated that the knockdown of USP36 induced extra apoptosis in CRC cells (Figures 3G, 3H). Finally, transwell assay data suggested that the migration and invasion of CRC cells were remarkably attenuated by USP36 knockdown (Figures 3I–3L). These results collectively underscore the critical role of USP36 in promoting CRC progression.

**USP36 regulates the stemness of CRC cells.** To assess the role of USP36 in maintaining stemness of CRC cells, we initially conducted colony formation assay and the results

revealed a significant reduction in the number of colonies derived from USP36-deficient CRC cells compared to control CRC cells (Figures 4A, 4B). Next, we performed sphere formation assays and the data showed that the size of spheres developed from USP36-deficient CRC cells was significantly smaller than that developed from control CRC cells (Figures 4C, 4D). Subsequently, we examined CSC markers CD144 and EpCAM by flow cytometry and the data demonstrated a dramatic decrease in the expression of CD144 and EpCAM in USP36-depleted CRC cells (Figures 4E, 4F). Finally, we evaluated the expression of pluripotent transcrip-

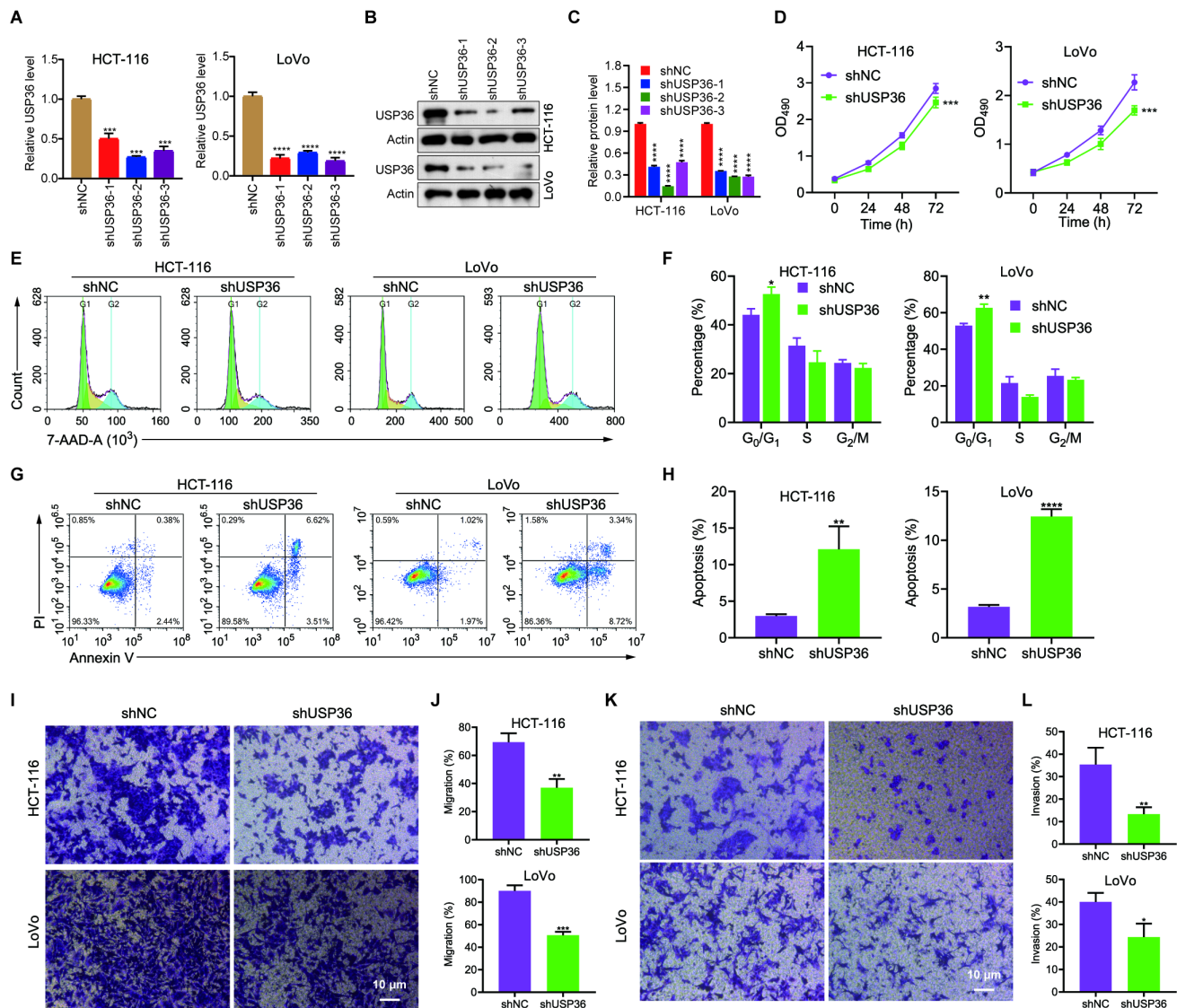


**Figure 3.** The role of USP36 in CRC cells. **A)** RT-qPCR data showing the USP36 knockdown efficiency in HCT-116 and LoVo cells. **B)** Western blotting results indicating USP36 expression in HCT-116 and LoVo cells transfected with shUSP36s or shNC. **C)** Quantification of the western blotting data. **D)** MTT assay outcomes depicting the viability of control and USP36-depleted CRC cells. **E)** 7-AAD staining results illustrating the cell cycle status of control and USP36-depleted CRC cells. **F)** Quantification of the 7-AAD staining results shown in E. **G)** Annexin V/PI staining data indicating the apoptosis of control and USP36-depleted CRC cells. **H)** Quantification of the data in G. **I)** Transwell assay data measuring the migration of control and USP36-depleted CRC cells. **J)** Quantification of the data in I. **K)** Transwell assay results showing the invasion of control and USP36-depleted CRC cells. \* $p < 0.05$ , \*\* $p < 0.01$ , \*\*\* $p < 0.001$ , \*\*\*\* $p < 0.0001$

tion factors, including OCT4, SOX2, NANOG, and MYC, which are also expressed by CSC [25, 26]. Western blotting data uncovered that USP36 knockdown resulted in a significant decrease of OCT4, MYC, NANOG, and SOX2 expression in CRC cells (Figures 4G, 4H). These results indicate that USP36 controls the stemness of CRC cells.

**Discussion**

In this study, we explored the role of USP36 in CRC. USP36 was initially identified and characterized in ovarian cancer cells [27]. Previous studies have demonstrated that knockdown of USP36 can suppress proliferation and induce apoptosis in various cancers, including glioblastoma, esophageal squamous carcinoma, and non-small cell lung cancer [19, 28, 29]. Additionally, USP36 has been reported to regulate tumorigenesis, drug sensitivity, and mitochondrial oxidative stress by controlling protein stability, such as ALKBH5, c-MYC, SOD2, and YAP [14, 19, 29, 30]. Consis-

tent with the oncogenic role of USP36 in other cancers, our data that USP36 is overexpressed in CRC and predicts poor prognosis of CRC patients, and that knockdown of USP36 in CRC cells resulted in reduced viability, cell cycle arrest, increased apoptosis, as well as attenuated cell migration and invasion strongly suggest that USP36 is an oncogene in CRC as well. Nevertheless, how USP36 controls these activities in CRC cells remains unclear. It would be interesting to identify the targets of USP36 in CRC cells.

USPs have been demonstrated to maintain the stemness of CSC in multiple cancers. For example, USP2 maintains CSC in breast cancer by activating Bmi1 and Twist [31]. USP22 maintains the stemness of CSC in gastric cancer by stabilizing BMI1 [32]. Consistently, our GSEA results showed that USP36 expression is linked to the Notch and Hedgehog pathways, which are crucial for maintaining CSC stemness [33]. Moreover, our data showed that USP36 depletion reduced the expression of CSC markers and pluripotent transcription factors and impaired the stemness of CRC

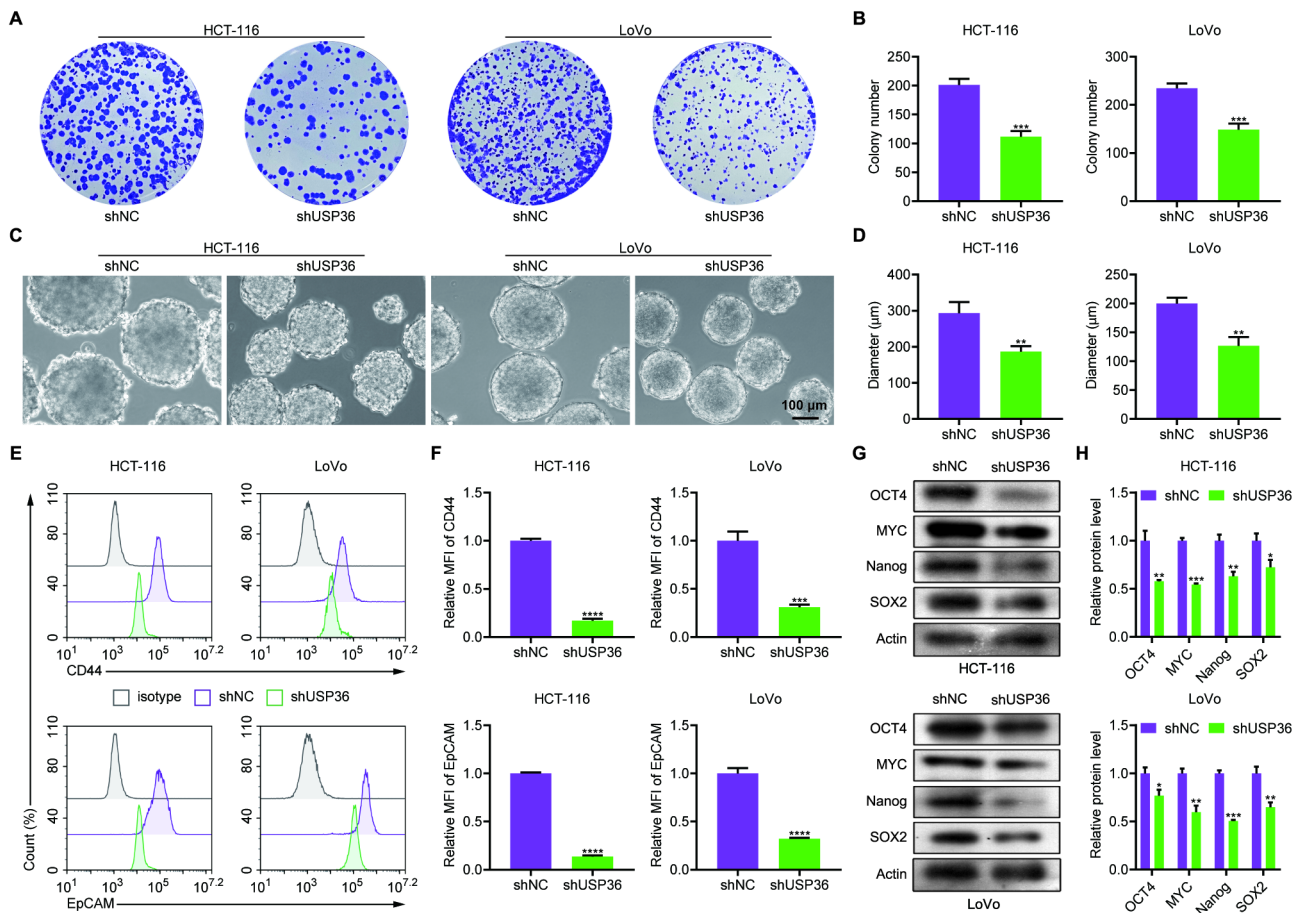


**Figure 4.** USP36 regulates the stemness of CRC cells. A) Colony formation assay data showing the clonogenicity of control and USP36-deficient HCT-116 and LoVo cells. B) Quantification of the data presented in A. C) Sphere formation assay results depicting the morphology of spheres derived from control and USP36-deficient CRC cells. D) Quantification of the results shown in C. E) Flow cytometry analysis outcomes illustrating the expression of CD44 and EpCAM in control and USP36-deficient CRC cells. F) Quantification of the data shown in E. G) Western blot results indicating the protein levels of OCT4, MYC, NANOG, and SOX2 in CRC cells. \*p<0.05, \*\*p<0.01, \*\*\*p<0.001, \*\*\*\*p<0.0001

cells. These observations underscore USP36 as another USP regulating the stemness of CSC. However, whether USP36 fulfills this function through modulating the Notch and Hedgehog pathways needs further investigation.

In conclusion, our findings offer valuable insights into the oncogenic role of USP36 in CRC, highlighting it as a potential target for CRC treatment.

**Acknowledgments:** This work was supported by the Startup Fund for Scientific Research, Fujian Medical University (Grant numbers 2021QH1259).

## References

- [1] SIEGEL RL, MILLER KD, JEMAL A. Cancer statistics, 2016. *CA Cancer J Clin* 2016; 66: 7–30. <https://doi.org/10.3322/caac.21332>
- [2] FERLAY J, SOERJOMATARAM I, DIKSHIT R, ESER S, MATHERS C et al. Cancer incidence and mortality worldwide: sources, methods and major patterns in GLOBOCAN 2012. *Int J Cancer* 2015; 136: E359–386. <https://doi.org/10.1002/ijc.29210>
- [3] SIEGEL RL, MILLER KD, GODING SAUER A, FEDEWA SA, BUTTERLY LF et al. Colorectal cancer statistics, 2020. *CA: a Cancer Journal For Clinicians* 2020; 70: 145–164. <https://doi.org/10.3322/caac.21601>
- [4] DE SOUSA E MELO F, KURTOVA AV, HARNOSS JM, KLJAVIN N, HOECK JD et al. A distinct role for Lgr5(+) stem cells in primary and metastatic colon cancer. *Nature* 2017; 543: 676–680. <https://doi.org/10.1038/nature21713>
- [5] CLARA JA, MONGE C, YANG Y, TAKEBE N. Targeting signalling pathways and the immune microenvironment of cancer stem cells – a clinical update. *Nat Rev Clin Oncol* 2020; 17: 204–232. <https://doi.org/10.1038/s41571-019-0293-2>
- [6] HAN J, WON M, KIM JH, JUNG E, MIN K et al. Cancer stem cell-targeted bio-imaging and chemotherapeutic perspective. *Chem Soc Rev* 2020; 49: 7856–7878. <https://doi.org/10.1039/d0cs00379d>
- [7] VERMEULEN L, TODARO M, DE SOUSA MELLO F, SPRICK MR, KEMPER K et al. Single-cell cloning of colon cancer stem cells reveals a multi-lineage differentiation capacity. *Proc Natl Acad Sci U S A* 2008; 105: 13427–13432. <https://doi.org/10.1073/pnas.0805706105>
- [8] YANG L, SHI P, ZHAO G, XU J, PENG W et al. Targeting cancer stem cell pathways for cancer therapy. *Signal Transduct Target Ther* 2020; 5: 8. <https://doi.org/10.1038/s41392-020-0110-5>
- [9] BAYIK D, LATHIA JD. Cancer stem cell-immune cell cross-talk in tumour progression. *Nat Rev Cancer* 2021; 21: 526–536. <https://doi.org/10.1038/s41568-021-00366-w>
- [10] HUANG T, SONG X, XU D, TIEK D, GOENKA A et al. Stem cell programs in cancer initiation, progression, and therapy resistance. *Theranostics* 2020; 10: 8721–8743. <https://doi.org/10.7150/thno.41648>
- [11] BAJAJ J, DIAZ E, REYA T. Stem cells in cancer initiation and progression. *J Cell Biol* 2020; 219. <https://doi.org/10.1083/jcb.201911053>
- [12] TAILLEBOURG E, GREGOIRE I, VIARGUES P, JACOMIN AC, THEVENON D et al. The deubiquitinating enzyme USP36 controls selective autophagy activation by ubiquitinated proteins. *Autophagy* 2012; 8: 767–779. <https://doi.org/10.4161/aut.19381>
- [13] YAN Y, XU Z, HUANG J, GUO G, GAO M et al. The deubiquitinase USP36 Regulates DNA replication stress and confers therapeutic resistance through PrimPol stabilization. *Nucleic Acids Res* 2020; 48: 12711–12726. <https://doi.org/10.1093/nar/gkaa1090>
- [14] SUN XX, HE X, YIN L, KOMADA M, SEARS RC et al. The nucleolar ubiquitin-specific protease USP36 deubiquitinates and stabilizes c-Myc. *Proc Natl Acad Sci U S A* 2015; 112: 3734–3739. <https://doi.org/10.1073/pnas.1411713112>
- [15] ANTA B, MARTÍN-RODRÍGUEZ C, GOMIS-PEREZ C, CALVO L, LÓPEZ-BENITO S et al. Ubiquitin-specific Protease 36 (USP36) Controls Neuronal Precursor Cell-expressed Developmentally Down-regulated 4-2 (Nedd4-2) Actions over the Neurotrophin Receptor TrkA and Potassium Voltage-gated Channels 7.2/3 (Kv7.2/3). *J Biol Chem* 2016; 291: 19132–19145. <https://doi.org/10.1074/jbc.M116.722637>
- [16] KAHROBA H, RAMEZANI B, MAADI H, SADEGHI MR, JABERIE H et al. The role of Nrf2 in neural stem/progenitors cells: From maintaining stemness and self-renewal to promoting differentiation capability and facilitating therapeutic application in neurodegenerative disease. *Ageing Res Rev* 2021; 65: 101211. <https://doi.org/10.1016/j.arr.2020.101211>
- [17] ZHAO H, MING T, TANG S, REN S, YANG H et al. Wnt signaling in colorectal cancer: pathogenic role and therapeutic target. *Mol Cancer* 2022; 21: 144. <https://doi.org/10.1186/s12943-022-01616-7>
- [18] ZHU S, HOU S, LU Y, SHENG W, CUI Z et al. USP36-Mediated Deubiquitination of DOCK4 Contributes to the Diabetic Renal Tubular Epithelial Cell Injury via Wnt/ $\beta$ -Catenin Signaling Pathway. *Front Cell Dev Biol* 2021; 9: 638477. <https://doi.org/10.3389/fcell.2021.638477>
- [19] CHANG G, XIE GS, MA L, LI P, LI L et al. USP36 promotes tumorigenesis and drug sensitivity of glioblastoma by deubiquitinating and stabilizing ALKBH5. *Neuro Oncol* 2023; 25: 841–853. <https://doi.org/10.1093/neuonc/noac238>
- [20] ROBINSON MD, MCCARTHY DJ, SMYTH GK. edgeR: a Bioconductor package for differential expression analysis of digital gene expression data. *Bioinformatics* 2010; 26: 139–140. <https://doi.org/10.1093/bioinformatics/btp616>
- [21] REIMAND J, ISSERLIN R, VOISIN V, KUCERA M, TANNUS-LOPES C et al. Pathway enrichment analysis and visualization of omics data using g: Profiler, GSEA, Cytoscape and EnrichmentMap. *Nat Protoc* 2019; 14: 482–517. <https://doi.org/10.1038/s41596-018-0103-9>
- [22] BAHMAD HF, CHEAITO K, CHALHOUB RM, HADADEH O, MONZER A et al. Sphere-Formation Assay: Three-Dimensional in vitro Culturing of Prostate Cancer Stem/Progenitor Sphere-Forming Cells. *Front Oncol* 2018; 8: 347. <https://doi.org/10.3389/fonc.2018.00347>
- [23] MA XL, SUN YF, WANG BL, SHEN MN, ZHOU Y et al. Sphere-forming culture enriches liver cancer stem cells and reveals Stearoyl-CoA desaturase 1 as a potential therapeutic target. *BMC Cancer* 2019; 19: 760. <https://doi.org/10.1186/s12885-019-5963-z>

- [24] PASTRANA E, SILVA-VARGAS V, DOETSCH F. Eyes wide open: a critical review of sphere-formation as an assay for stem cells. *Cell Stem Cell* 2011; 8: 486–498. <https://doi.org/10.1016/j.stem.2011.04.007>
- [25] CHAUDHARY A, RAZA SS, HAQUE R. Transcriptional factors targeting in cancer stem cells for tumor modulation. *Semin Cancer Biol* 2023; 88: 123–137. <https://doi.org/10.1016/j.semcancer.2022.12.010>
- [26] LIU A, YU X, LIU S. Pluripotency transcription factors and cancer stem cells: small genes make a big difference. *Chin J Cancer* 2013; 32: 483–487. <https://doi.org/10.5732/cjc.012.10282>
- [27] KIM MS, KIM YK, KIM YS, SEONG M, CHOI JK et al. Deubiquitinating enzyme USP36 contains the PEST motif and is polyubiquitinated. *Biochem Biophys Res Commun* 2005; 330: 797–804. <https://doi.org/10.1016/j.bbrc.2005.03.051>
- [28] DENG Q, WU M, DENG J. USP36 promotes tumor growth of non-small cell lung cancer via increasing KHK-A expression by regulating c-MYC-hnRNPH1/H2 axis. *Hum Cell* 2022; 35: 694–704. <https://doi.org/10.1007/s13577-022-00677-6>
- [29] ZHANG W, LUO J, XIAO Z, ZANG Y, LI X et al. USP36 facilitates esophageal squamous carcinoma progression via stabilizing YAP. *Cell Death Dis* 2022; 13: 1021. <https://doi.org/10.1038/s41419-022-05474-5>
- [30] KIM MS, RAMAKRISHNA S, LIM KH, KIM JH, BAEK KH. Protein stability of mitochondrial superoxide dismutase SOD2 is regulated by USP36. *J Cell Biochem* 2011; 112: 498–508. <https://doi.org/10.1002/jcb.22940>
- [31] HE J, LEE HJ, SAHA S, RUAN D, GUO H et al. Inhibition of USP2 eliminates cancer stem cells and enhances TNBC responsiveness to chemotherapy. *Cell Death Dis* 2019; 10: 285. <https://doi.org/10.1038/s41419-019-1512-6>
- [32] MA Y, FU HL, WANG Z, HUANG H, NI J et al. USP22 maintains gastric cancer stem cell stemness and promotes gastric cancer progression by stabilizing BMI1 protein. *Oncotarget* 2017; 8: 33329–33342. <https://doi.org/10.18632/oncotarget.16445>
- [33] NWABO KAMDJE AH, TAKAM KAMGA P, TAGNE SIMO R, VECCHIO L, SEKE ETET PF et al. Developmental pathways associated with cancer metastasis: Notch, Wnt, and Hedgehog. *Cancer Biol Med* 2017; 14: 109–120. <https://doi.org/10.20892/j.issn.2095-3941.2016.0032>